PIT Project

**Behaviour of steel framed structures under fire conditions**

# British Steel Fire Test1:
# Reference ABAQUS model using grillage representation for slab

## Research Report

**Report R99-MD1**

Abdel Moniem Sanad

**The University of Edinburgh**
**School of Civil & Environmental Engineering**
**Edinburgh, UK**

**December, 1999**

# TABLE OF CONTENTS

## LIST OF FIGURES :



**NOTES:**

1. In the description of the numerical model below we use the following terms :
2. “the plane” to define the plane of the floor.
3. “joist” means a steel beam, and the “test joist” means the heated joist during the fire test.
4. “vertical” means vertical to the slab plane.
5. “in-plane” means in the plane of the slab.
6. “joist longitudinal direction” or “longitudinal direction” to mean parallel to the joist length coordinate.
7. “transverse direction” to mean at right angle to the joist longitudinal direction (i.e. in the direction of the longitudinal axis of the ribs).
8. “Reference vertical coordinate” is the interface between the slab and joist.

# Description of finite element model for

# Cardington first fire test

## 1. GEOMETRIC DESCRIPTION

### 1.1. Layout

The test was performed on the seventh floor of the building. The fire compartment was arranged to study the behaviour of a secondary beam.spanning between two columns. The dimension of the compartment was 8mx3m. The tested beam was of 9m span connected semi-rigidly to columns at either end. A standard composite profiled deck slab was used to span the 3m between equally spaced secondary beams connected to colums or primary beams (also spanning 9m).

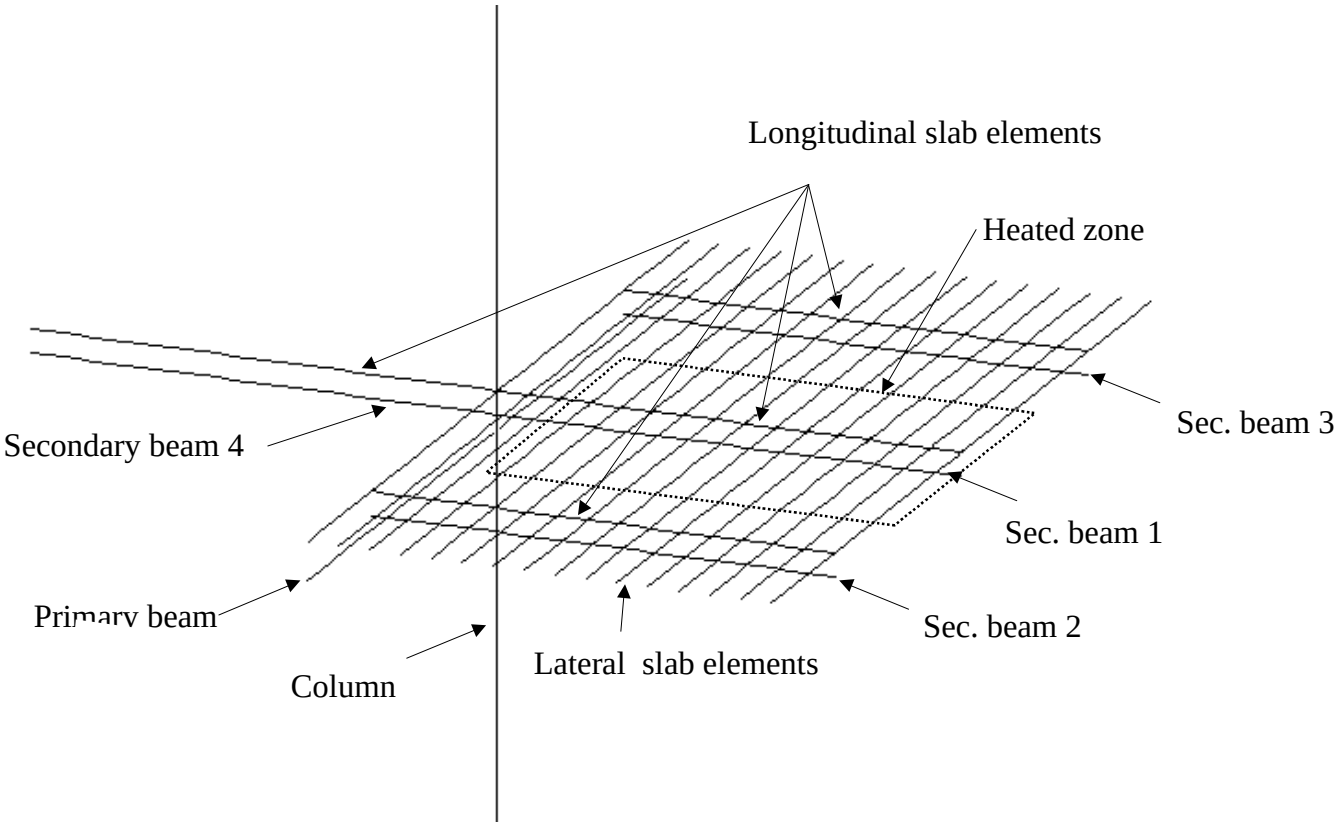


Model of fire test1

**Figure 1**

### 1.2. Finite element mesh

Figure 1 shows the finite element model of the test. The area affected by the fire is indicated by dashed lines. In the direction of the heated beam (longitudinal), the model extends from the centre of the heated compartment to the column and continues to the centre of the adjacent compartment.

In the transverse direction, the model extends 4.5m on either side of the heated beam (to centreline of the next slab span). In the model, each structural steel member is idealized by an appropriate beam element. Figure 2 shows the typical cross-section of the steel members and table I, gives the dimensions of the column, primary and secondary beams respectively. The centroid of the secondary joists is located 152.5mm below the reference vertical coordinate of the joist's top flange. The column is modelled using a similar beam elements.

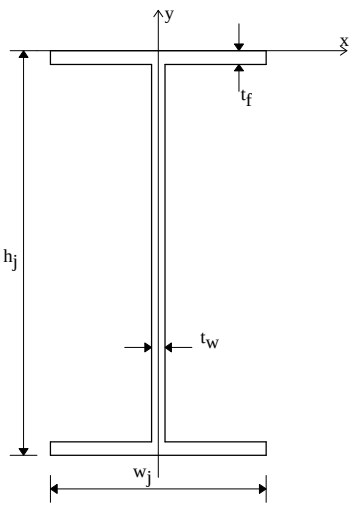


Typical cross section of the steel beams

**Figure 2**

| | $h_j$ (mm) | $w_j$ (mm) | $t_f$ (mm) | $t_w$ (mm) |
|---|---|---|---|---|
| **Column** | 260.2 | 255.9 | 17.3 | 10.6 |
| **Primary beams** | 602 | 301 | 14.8 | 10.6 |
| **Secondary beams** | 303.8 | 151.9 | 10.2 | 6.1 |

**Table 1**

Dimensions of the steel members

The slab behaviour is modelled by a grillage type idealization using beam elements to represent the slab behaviour in both the longitudinal and transverse directions. In the longitudinal direction, the slab element has a rectangular section with 70mm depth and an effective width equal to 2250mm, calculated according to the Eurocode 4 (ENV1994) for a simply supported beam case. In the transverse direction, slab elements have a trapezoidal shape and the geometry of the concrete section in this direction is shown in figure 3. The thickness of the steel deck used is 9mm. Reinforcement of one layer of A142 mesh was provided. Table 2 gives the dimensions of the sections in both directions.

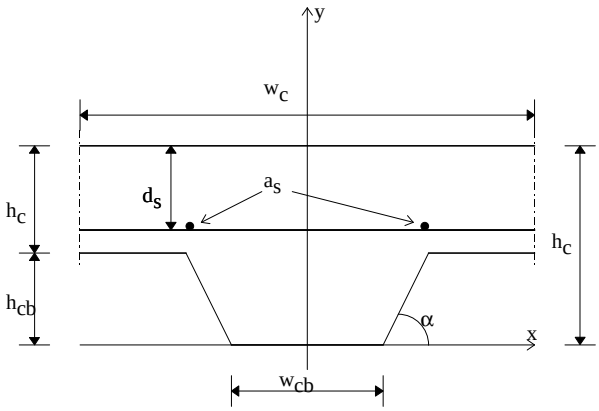


Cross section of the composite slab

**Figure 3**

| | $w_c$ mm | $w_{cb}$ mm | $h_{ct}$ mm | $h_{cb}$ mm | α (°) | $a_s$ mm$^2$ | $d_s$ mm |
|---|---|---|---|---|---|---|---|
| **Slab in transverse direction** | 300 | 136 | 70 | 60 | 65 | 42.6 | 55 |
| **Slab in longitudinal direction** | 2250 | - | 70 | - | - | 319.5 | 55 |

**Table 2**

Dimensions of slab sections

## 2. MATERIAL BEHAVIOUR

For steel structures under high temperature the relationship between stress and strain changes considerably. At increased temperature, the material properties degrade and it's capacity to deform increases which is measured by the reduction of the Young's modulus. In the finite element model, the relation between the stress and the strain under high temperature is defined according to the Eurocode 3 (ENV1993). The relation is elastic-perfect plastic at ambient temperature, and the reduction of the material properties starts at a temperature higher than 100C as shown in figure 4. Identical material behaviour is assumed for both tension and compression.

Similarly, the behaviour of concrete is characterised by material property degradation with increased temperature. The stress-strain relationship is then defined according to the Eurocode 2 (ENV1992) as shown in figure 5. Here, the initial elastic behaviour is followed by a plastic hardening curve up to the ultimate stress, after which, a decaying zone represents the post-crushing behaviour for concrete. This relationship has the advantage of allowing the definition of a stress level for large plastic deformations, usually reached during fire conditions. It may be noted that no tension is considered in the model for the concrete at both ambient and elevated temperature, however the tensile resistance of the reinforcement and the steel deck is considered.

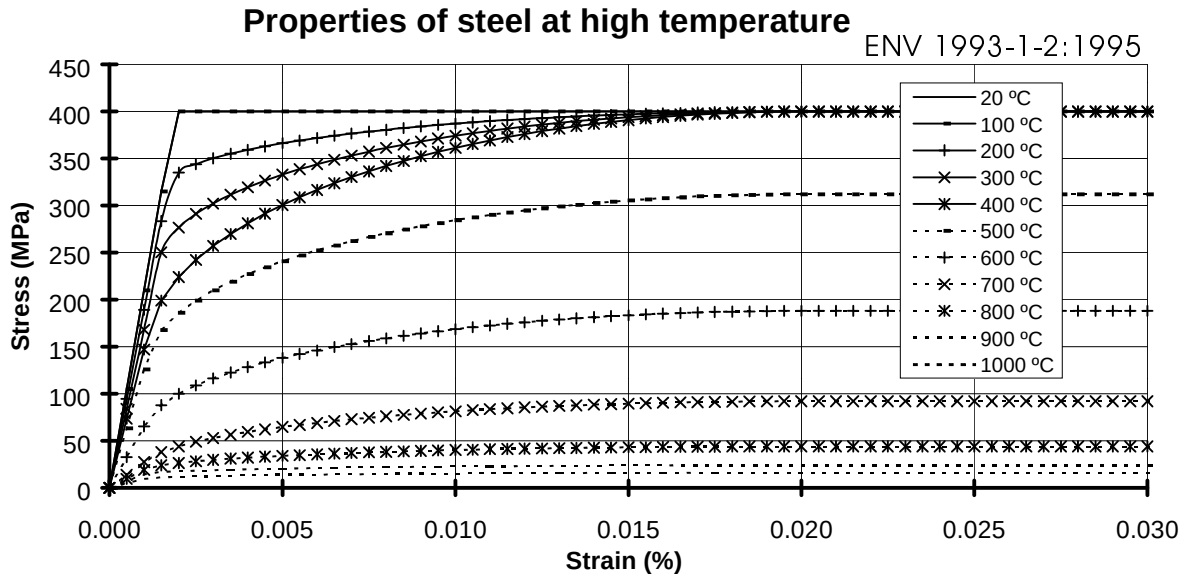


**Figure 4**

Steel stress-strain relationship at high temperature

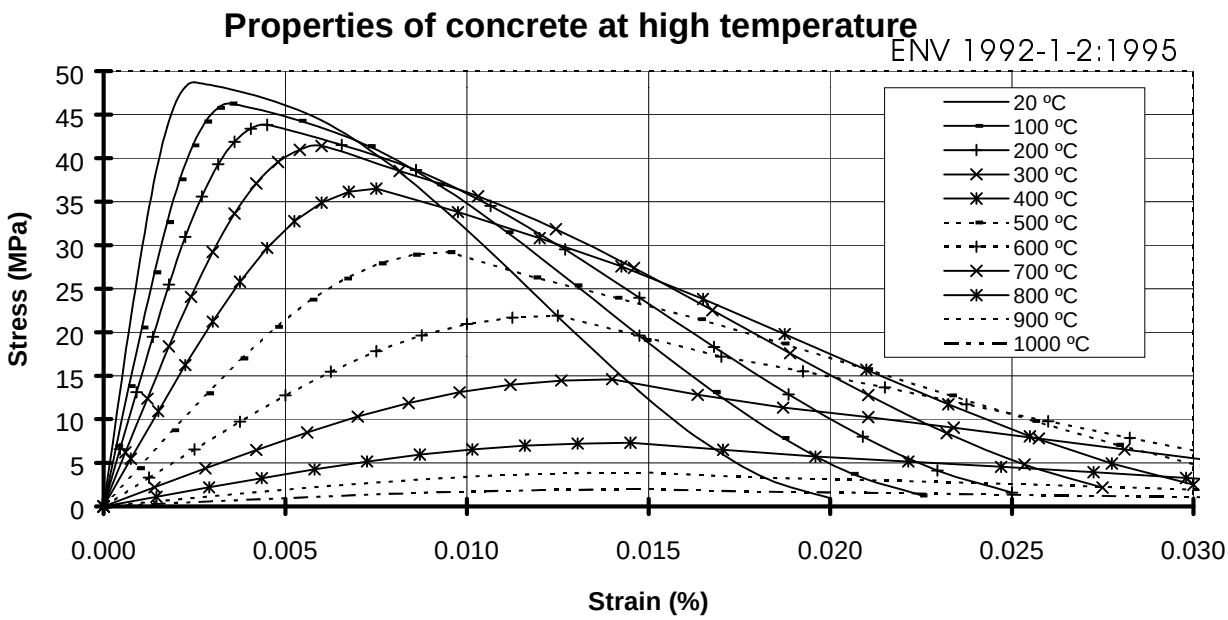


**Figure 5**

Concrete stress-strain relationship at high temperature

## 2.1. Section behaviour for steel members

For all steel members, the classic linear beam element applying the hypotheses of *plane surface remains plane* is used. Each point on the cross section, along each member, follows the stress-strain relationship (figure 4) as a function of the point's temperature. This takes into consideration the

variable temperature profile applied across the section and the corresponding material properties during different stages of the fire. The connections between different steel members (beam to column connection and beam to beam connection) are modelled by rigid connections where boundary conditions are imposed on the relative displacement of the joining elements.

## 2.2. Slab modelling

In a reinforced concrete slab, more complex behaviour has to be modelled. The different behaviour of concrete in tension and compression, the orthotropic behaviour of concrete due to the reinforcing mesh and the decking steel and the development of membrane action need to be considered in order to provide a realistic representation of the slab behaviour. In the numerical model developed in this paper, the concrete modelling is based on the global behaviour of the concrete section, with the above factors taking into consideration. The slab is modelled by two sets of beam elements running parallel and perpendicular to the secondary beams. In each direction, the beam elements, have a pre-defined force-strain and moment-curvature relationship. These relationships are calculated based on the geometry and the material properties of the section in each direction and taking into account the variable temperature over the same section and the corresponding material properties (O'Connor and al. 1995).

The behaviour of the slab in the longitudinal direction (direction of the joist longitudinal axis) is modelled by beam elements, using bilinear moment/curvature and force/strain relationships which are uncoupled (figure6,7). The yield points for the force relationship in each sense are given by the section's plastic resistance for normal force (with different values for tension and compression). The yield points for the bending relationship are given by the section's plastic resistance for bending (with different values for sagging and hogging). The post-yield behaviour is modelled by a linear relationship (moment/curvature and force/strain), decreasing from the yield point to the ultimate section resistance based on the steel reaching the limiting strain for yield strength.

The behaviour of the slab in the direction normal to the joist (transverse) is modelled by beam elements. The transverse bending and transverse membrane action of the slab is modelled by beam elements with their longitudinal axis in the transverse direction, using bilinear moment/curvature and force/strain relationships which are uncoupled (figure8,9). The yield points for the force relationship in each sense are given by the section's plastic resistance for normal force (with different values for tension and compression). The yield points for the bending relationship are given by the section's plastic resistance for bending (with different values for sagging and hogging). These beam ribs have a very high bending stiffness about a vertical axis (i.e. relating to bending deformations in the horizontal plane) to ensure that the membrane shear stiffness of the slab is represented (that is: this bending stiffness is 100 times the value for bending of an individual rib). The beam used in modelling the slab are 3D beam element which has torsional and weak axis bending properties, with linear elastic behaviour for both the torsional and the bending about the weak axis.

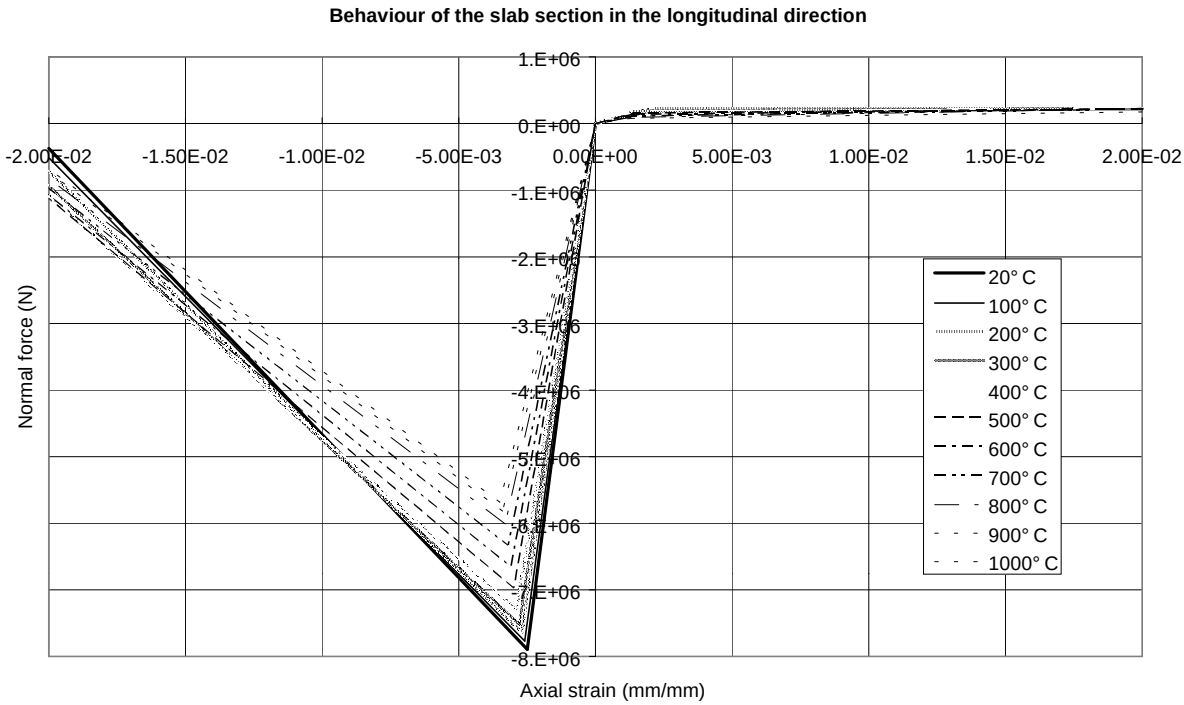


**Figure 6**

Axial Force- Axial Strain relationship at high temperature in the longitudinal direction

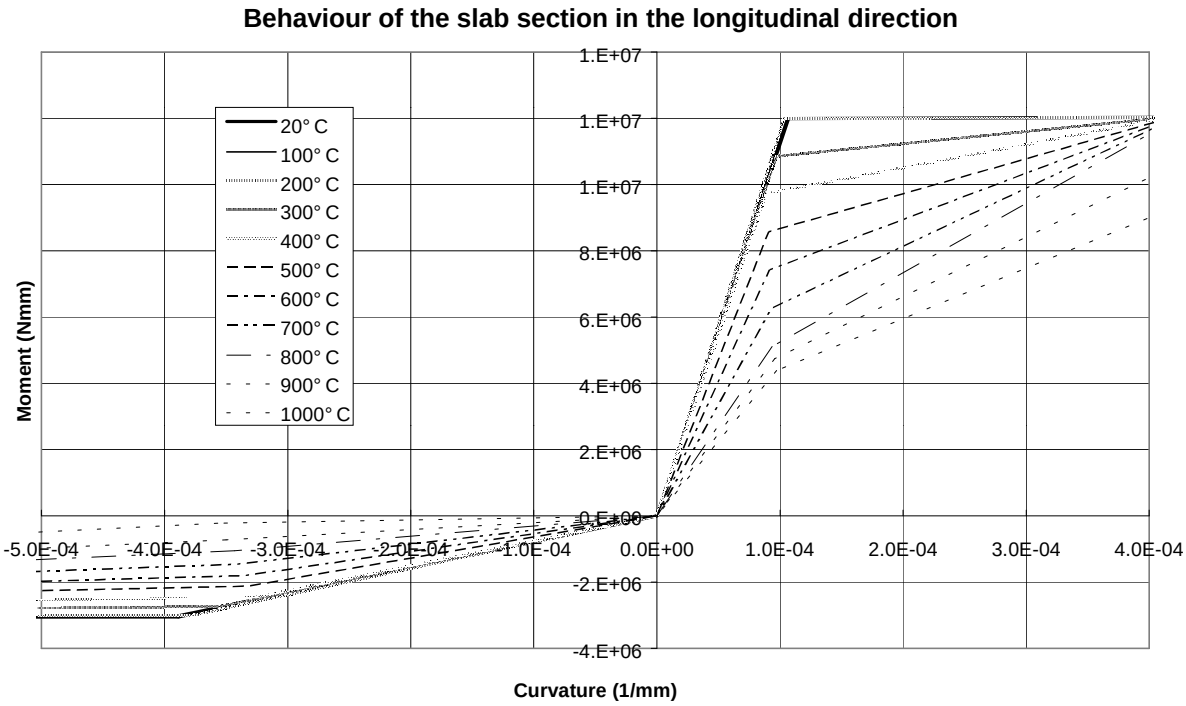


**Figure 7**

Moment-Curvature relationship at high temperature in the longitudinal direction

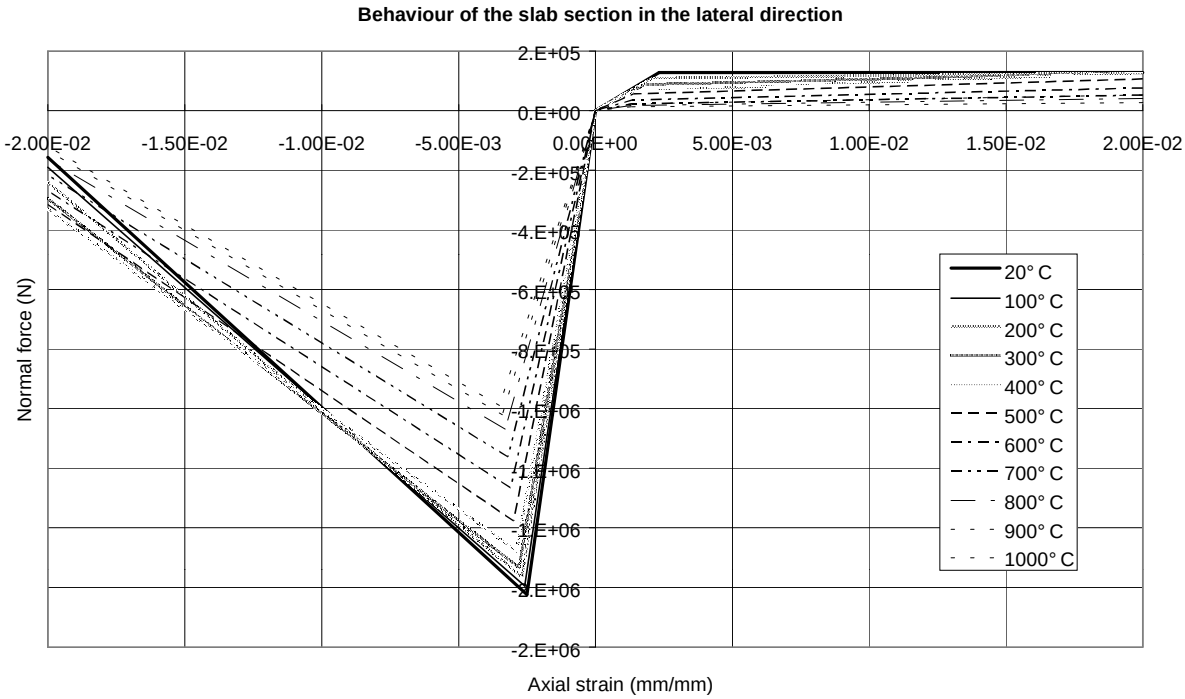


**Figure 8**

Axial Force- Axial Strain relationship at high temperature in the lateral direction

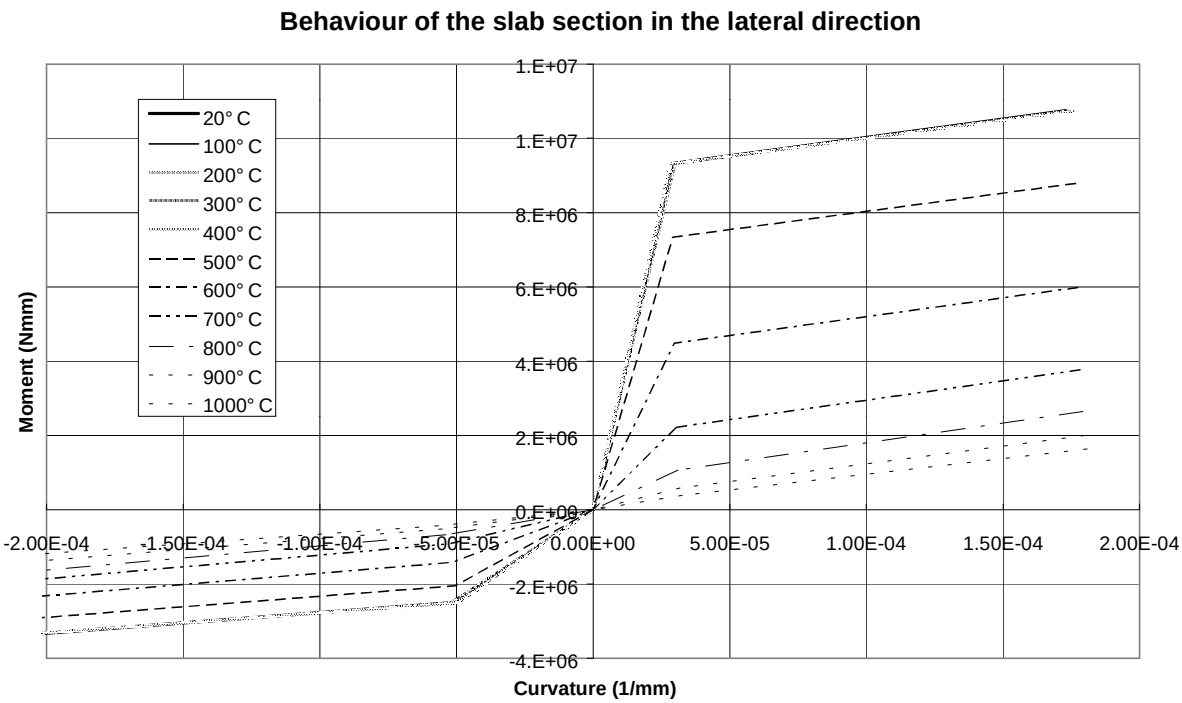


**Figure 9**

Moment-Curvature relationship at high temperature in the lateral direction

## 3. CONNECTIONS BETWEEN MEMBERS

The beam models for the longitudinal and transverse action of the slab (ribs) are connected to the joist only at the crossing points using rigid beam type connection. This provide a rigid beam between two nodes to constrain the displacement and rotation of the slab's node to the displacement and rotation of the joist's node, corresponding to the presence of a rigid beam between the two nodes. The vertical separation of the joist centroid and the longitudinal slab is properly modelled. The centroid of the longitudinal slab is taken as 35mm below the slab surface and the thickness of the longitudinal slab as 70mm. The effective width of the longitudinal slab is taken as 2250mm throughout the length of the beam.

The vertical separation between the joist centroid and the transverse slab is properly represented, with the centroid of the transverse ribs taken as 55mm below the slab surface. Each of the two secondary beams (joists) which run parallel to the heated joist has a composite slab connected to it. The end of the each secondary beams (joists) is connected to the primary beams (joists), which has a composite slab connected to it as well.

The secondary beam (joist) opposite to the tested joist (beyond the column on the same axe as the test joist) is modelled by beam elements and has a composite slab connected to it. The tested secondary beam and the opposite secondary beam are connected to the column at the level of their centre line. The 2 primary beams are connected to the column at the level of their centre line. The effect of the slab beyond the column is modelled by applying boundary conditions, on the rotations and displacement of the primary beam, column, and secondary beam beyond the column.

## 4. BOUNDARY CONDITIONS

The column is completely fixed at it's bottom end and free to displace vertically at the top end. Column rotation about the vertical axe is fixed at the level of the connection with the secondary beams. For all secondary joists, symmetrical conditions are imposed at mid-span (Longitudinal displacement and rotation about transverse horizontal axis are fixed. Rotations about the vertical axe is fixed at mid span as well. For the primary beams; their far end are restrained against all rotations, and against vertical and lateral displacements. At the location of connection with the 2 secondary beams, rotation about the vertical and lateral (parallel to the primary beam) axes are restrained. The longitudinal displacement (parallel to the secondary beams) are restrained is restrained as well.

Each longitudinal slab is connected to a secondary beam (joist), thus have same boundary conditions as the joist below it (symmetrical conditions at mid-span). The longitudinal slab above the test joist is connected to the longitudinal slab over the adjacent joist (continuous over the column). The longitudinal slab above the secondary joists (parallel to the test joist) are connected to the longitudinal slab over the primary beam. For the transverse slab: the slab is treated as translationally and rotationally continuous over the test joist and over the two other secondary beams. The rotations about vertical and lateral directions are fixed at the far end points which are fixed against horizontal displacement in the direction of the rib axis, and horizontal displacement normal to the rib axis. These points are free to move vertically (perpendicular to the plane of the slab). Figure 10 shows the boundary conditions used in the model. The symbolic one arrow indicates a displacement restraint in the arrow direction and two arrows indicates a rotational restraint around the arrow direction.

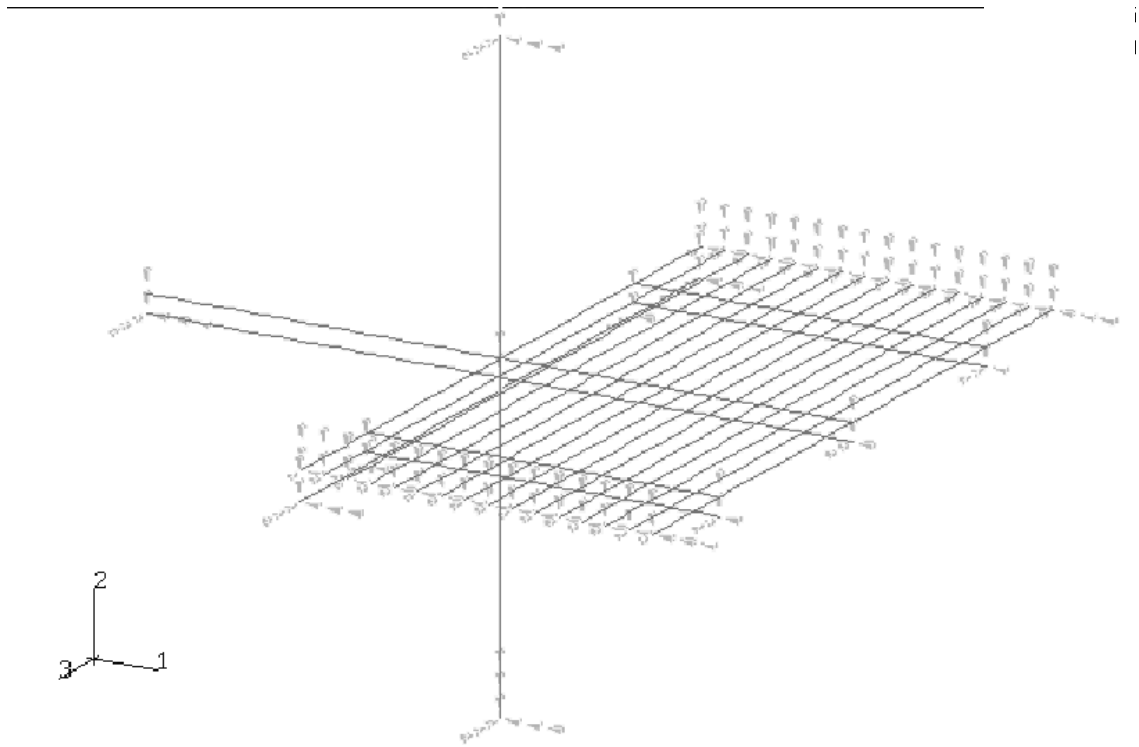


**Figure 10**

Boundary conditions in the numerical model

## 5. LOADING

### 5.1. Distributed load

The self weight of the structure and the live load applied during the test are combined to give an imposed floor load of 5.48KN/m$^2$. In the numerical model a distributed load of 5.48 kPa is applied to the slab by means of the uniformly distributed loads on the ribs of 1.644 kN/m. This is maintained at constant value throughout the thermal loading process. Non linear geometric and material effects were modelled based on the large deformation theory using the Newton-Raphson method.

### 5.2. Thermal load

The effect of fire on the structure is modelled by increasing the temperature linearly from ambient temperature to the maximum temperature reached for each member respectively. The thermal effect on the structure was modelled by considering both, the expansion of each element and the thermal gradient across its section. These two factors are applied to the reinforced concrete slab as well as the joist. Thermal loading is applied only to the compartment heated zone and outside it according to the test measurements. It is applied by defining the final temperature (800°C a the joist centroid) and assuming a linear variation from the initial temperature (20°C) to the final temperature. The joist has temperature profile along its total length, and vertical variations in temperature are included as a vertical temperature gradient, following the test measurements. steel beam. Temperature gradients are modelled in both the slab and the joist. For the beam finite elements adopted here, the temperatures are defined as a centroidal temperature and a vertical difference between the extreme fibre and the centroid. The extreme fibre temperature of the lower flange of

the joist (LFT), which is used as the reference temperature here, is thus the combination of the input centroidal value and the gradient value.

For the slab, only the zone within the compartment is heated. The parts of the slab which lie outside the compartment zone are treated as remaining at ambient temperature at all times. The heating effect for the slab (membrane and gradient values) are applied both to the longitudinal slab and the transverse slab models separately. The temperature of all points in the slab which lie within the compartment are treated as equal at a given height within the slab. Each rib has a constant temperature over its heated length and is considered to be at ambient temperature outside the furnace. It may be noted here that the temperature applied to the slab is the mean temperature acting on its geometric centre and the gradient across its thickness is the mean gradient deduced from the temperature distribution calculated separately for the longitudinal and the transverse directions. Figure 11 shows an example of the measured temperature during the fire for the slab and the beam at mid span. In the model, the temperature of the beam varies from one location to another according to the measured temperatures. In this report the default temperature chosen to describe the different phenomena during the fire, is the temperature of the lower flange of the beam at mid span.

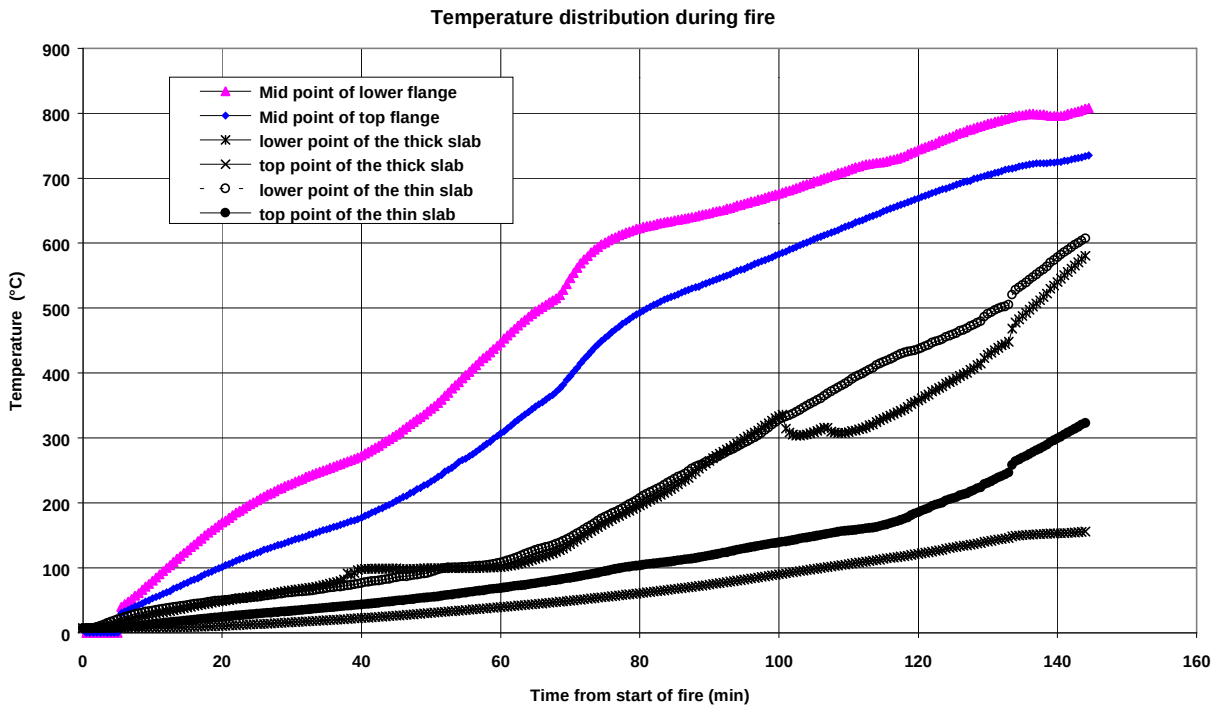


**Figure 11**

Temperatures in the tested beam and the slab during the fire

In the numerical model, the time lag between the test joist lower flange temperature and the upper flange temperature is represented by assuming a linear increase in the difference between the LFT and the UFT, starting from 0 at ambient temperature to 100°C at the maximum temperature (LFT=850°C). The relationship between the lower flange temperature (LFT = T1) and the slab centroidal temperature (SCT = T2) is characterised by a linear relationship with the following coordinates (T1,T2): (20,20), (800,360). The relationship between the lower flange temperature (LFT = T1) and the slab temperature gradient (SGT = DT3) is characterised by a linear relationship with the following coordinates (T1,DT3): (20,0), (800,5) (i.e. the centroidal temperature and the

gradient are arranged to give the top surface of the slab rising to 85 degrees at the end of the test, whilst the lower surface reaches 735°C when the lower flange temperature reaches 800°).

## 6. COMPARISON WITH TEST DATA

### 6.1. Deflection at mid-span

The first measurement point is located on the bottom flange of the beam at mid-span. Figure 12 shows the relation between the deflection of the beam at this point and the reference temperature of the lower flange at mid-span. At this location the reference temperature coincides with the temperature of the deflected point. The negative sign for the deflection indicates a vertical displacement downward. In both the finite element analysis and the experiment, the deflection increases with temperature and the experimental measurements show a relationship close to a straight line. In the finite element analysis the deflection starts increasing with a lower slope, compared to the test, up to 150°C then the relation becomes slightly non-linear reaching nearly the same final deflection value of 230mm at 850°C. The maximum difference between the model and the test is approximately 25mm and recorded near 400°C. The difference between the model and the test can be attributed to the difference in the temperature distribution applied over the slab in both cases. To be noted here that the measurment of temperature over the slab was insufficient to give a complete spatial distribution (only 4 location over the total heated zone).

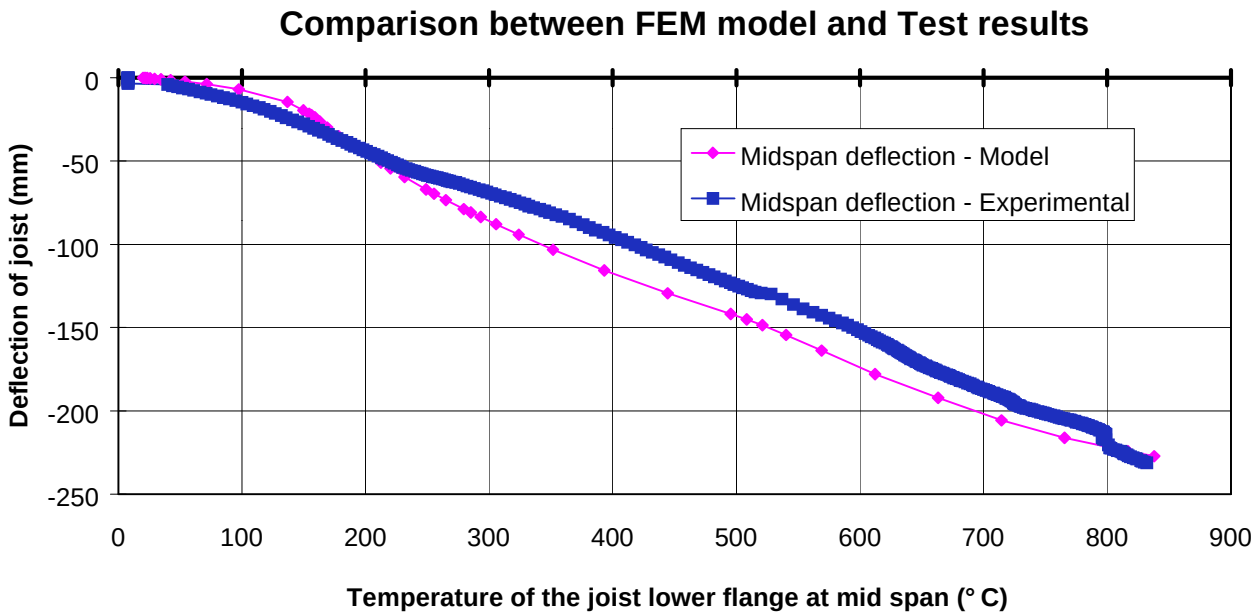


**Figure 12**

Deflection of the tested beam at midspan

### 6.2. Deflection at one third of span

The second point is located on the lower flange of the beam at 2.4m from the column. In figure 13, the deflection is plotted against the reference temperature of the lower flange at mid-span. Again the behaviour of the beam gives a linear relationship between the deflection and the reference temperature. Here the results from the numerical model can be divided into 3 parts. First zone, from ambient temperature until 150°C, the relation is linear and the slope is slightly smaller than the

experiment. The second zone, up to 400°C where the slope is higher than the test and the third zone where the numerical and the test results have the same slope. At this point the maximum difference between the model and the experiment is close to 25mm and recorded at 400°C. The maximum deflection reached at the end of the fire is 200mm in the numerical model against 180mm in the test. Here again the difference between the numerical and the test results can be attributed to the temperature distribution over the slab.

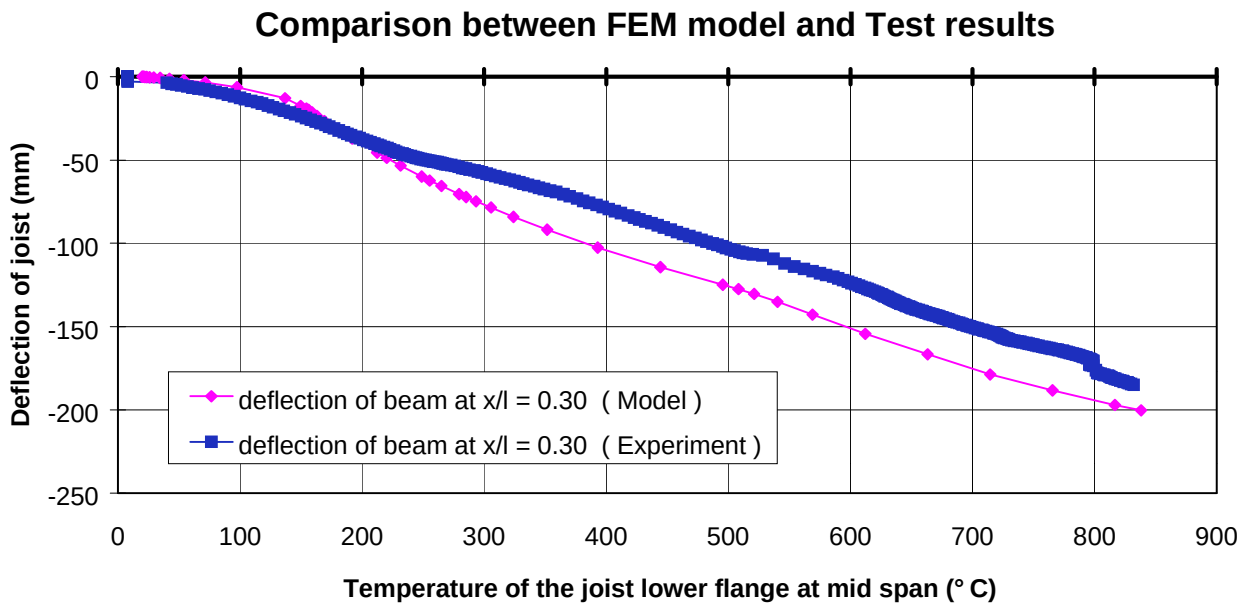


**Figure 13**

Deflection of the tested beam at 2.7m from column

### 6.3. Deflection at the limit of the heated zone

The third point is located just inside the heated zone, near the furnace wall, at 1.2m from the column. At this point of the beam the temperature rises up to 800°C. Figure 1414 shows the deflection of the lower flange at this point against the reference temperature. At this location, the numerical model and the experimental results curves are merged together up to 150°C, followed by a higher slope in the numerical model up to nearly 500°C, then both curves have a similar non linear tendency until the end of fire. The maximum difference between the two curves is nearly 20mm at 400°C and the final deflection reaches 63mm in the numerical model against 51mm in the test. At this location, just over the furnace wall, buckling occurred in the web of the beam between 400-500°C. This buckling was defined as 'material buckling' as it was related to the precipitous loss of material strength at high temperature. The numerical model in its actual configuration (using beam elements) can not predict local buckling, but it is able to calculate with good accuracy the change of stiffness in each structural element due to the reduction of the material properties over the element. However this local buckling which affects the local deflection at this point, seems to have a lesser effect on the global behaviour of the structure, in terms of the maximum deflection.

### 6.4. Deflection near the column

This point is located, in the non heated zone of the beam outside the furnace, at 0.3m from the column. The maximum temperature reached at this point is 220°C. Figure 15 shows the deflection

curve in the numerical and the experimental curves at this point. In the test, the deflection increases up to 16mm at 560°C (reference temperature) then it decreases and stabilises at 14mm. In the numerical model the deflection increases, in a non linear manner, and reaches a maximum value slightly higher then 6mm at 450°C then it decreases and stabilises just below 4mm. We can see that the predictions from the numerical model show a behaviour comparable to the test.

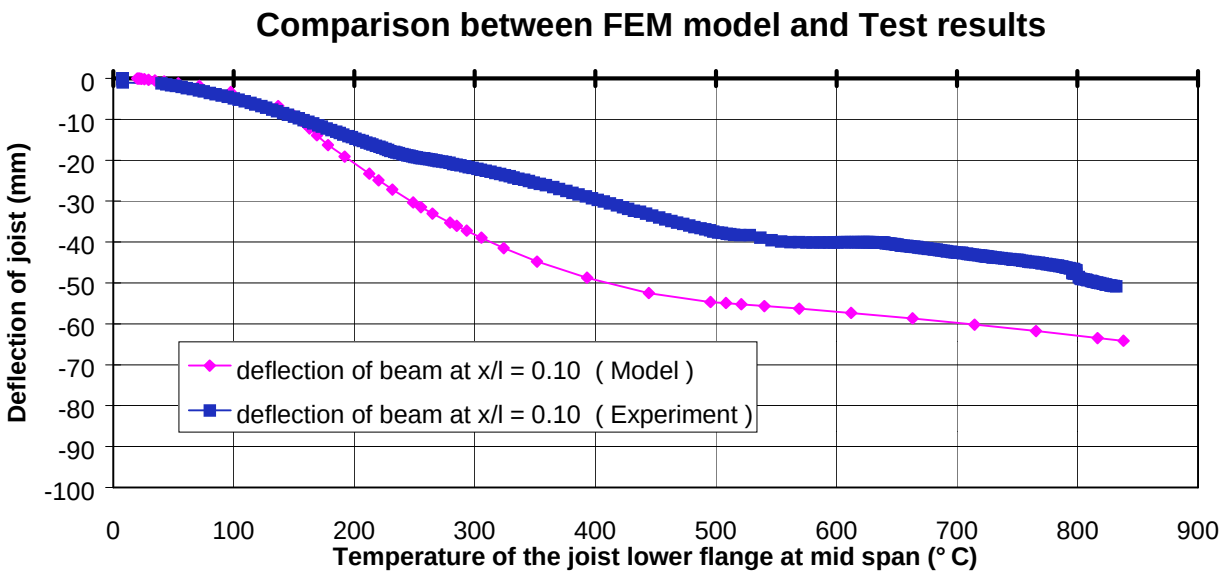


**Figure 14**

Deflection of the tested beam at 0.9m from column

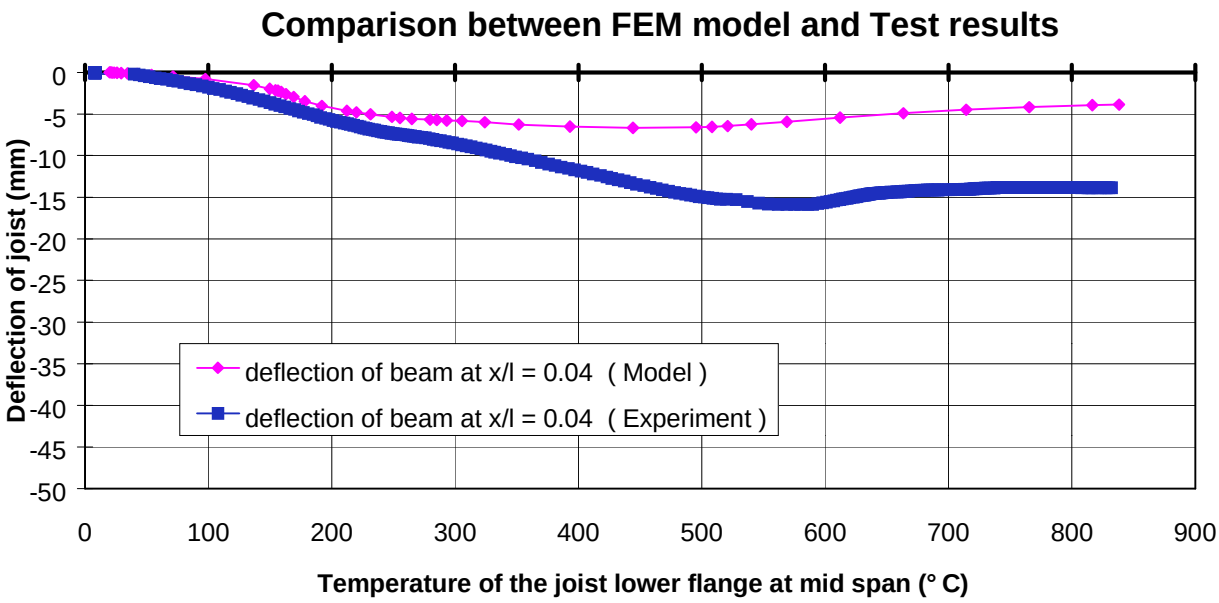


**Figure 15**

Deflection of the tested beam at 0.35 m from column

From the above comparisons, between the finite element predictions and the test measurements, we can see that the numerical model is in agreement with the test over the total time of the fire and the different approaches used in the model, described above, can predict with acceptable accuracy the global behaviour of the structure under fire conditions.

## 7. CONCLUSION

In this paper we described a finite element model developed to simulate the first full scale fire test carried in the large building test facility at Cardington. The test was dedicated to study the behaviour of a restrained composite beam under fire conditions. The composite action between the slab and the beam was assured in the model by means of rigid elements coinciding with the shear stud locations. The connections between different steel members were modelled by imposing displacement constraints to the nodes of the members. Using the general purpose finite element program ABAQUS, a numerical model capable of predicting the behaviour of the composite framed structures under fire condition was developed.

The results of the numerical model were compared with the experimental measurements at four different locations on the tested beam, inside and outwith the heated zone. The comparisons showed good agreement between the model and the test measurement for the total time of fire at different points of the tested beam. The finite element model developed in this paper has been developed with the aim of understanding local and global structural behaviour during fire. In the authors opinion redundant structure behaviour in fire is dominated by the effects of restrained thermal expansion and a variety of loadpaths are mobilised during the course of the loading. These issues are currently being explored through further application of the model described here and will be reported in greater detail in subsequent publications.

## 8. REFERENCES

Abaqus (1994) : Abaqus theory manual and users manual, version 5.4, Hibbit, Karlsson and Sorensen Inc., Pawtucket, Rhode Island, USA

P.N.R. Bravery (1993): Cardington large building test facility, Construction details for the first building, internal report British Steel plc.

D.J. O'Connor and al. (1995) : Determination of the fire endurance of model concrete slabs using a plastic analysis methodology, The Structural Engineer, Volume 73, No 19/3.

Eurocode 2 (1995) : Design of concrete structures - Part1-2 : General rules - Structural fire design, ENV 1992-1-2.

Eurocode 3 (1995) : Design of steel structures - Part1-2 : Fire resistance, ENV1993-1-2.

Eurocode 4 (1994) : Design of composite steel and concrete structures - Part1-1 : General rules and rules for buildings, ENV 1994-1-1.

B.R. Kirby (1995) : Behaviour of a multi-storey steel framed building subject to natural fires: Test1-restrained beam, deflection measurements, Document ref; S423/1/Part D1, British Steel plc.

B.R. Kirby (1995) : Behaviour of a multi-storey steel framed building subject to natural fires: Test1-restrained beam, temperature measurements, Document ref; S423/1/Part T1, British Steel plc.